

## Physicochemical Characterization of Microcrystalline Cellulose Extracted from Kenaf Bast

N. A. Sri Aprilia,<sup>a</sup> Y. Davoudpour,<sup>b</sup> W. Zulqarnain,<sup>b</sup> H. P. S Abdul Khalil,<sup>b,\*</sup> C. I. Che Mohamad Hazwan,<sup>b</sup> M. S. Hossain,<sup>c</sup> Rudi Dungani,<sup>d</sup> H. M. Fizree,<sup>b</sup> A. Zaidon,<sup>e</sup> and M. K. Mohamad Haafiz<sup>b</sup>

Microcrystalline cellulose (MCC) was successfully prepared from bleached kenaf bast fiber through hydrochloric acid hydrolysis. The influence of hydrolysis time (1 to 3 h) on the MCC physicochemical properties was examined. Scanning electron microscopy (SEM), X-ray diffraction (XRD), particle size analysis, Fourier transform infrared spectroscopy (FT-IR), and thermal gravimetric analysis (TGA) were utilized to characterize the isolated MCC. According to FTIR analysis, the chemical composition of MCC was not changed with the reaction time. The reaction times, however, did affect the thermal stability of MCC. The thermal stability decreased linearly with increasing hydrolysis time. The optimum hydrolysis time was determined based on the morphological, structural, and thermal properties of the kenaf bast MCC.

*Keywords:* Kenaf bast; Acid hydrolysis; Microcrystalline cellulose; Reaction time; Structural properties

*Contact information:* a: Department of Chemical Engineering, Engineering Faculty, University of Syiah Kuala, Banda Aceh, Indonesia; b: School of Industrial Technology, Universiti Sains Malaysia, 11800 USM, Penang, Malaysia; c: Malaysian Institute of Chemical & Bioengineering Technology, University of Kuala Lumpur, 78000 Alor Gajah, Melaka, Malaysia; d: School of Life Sciences and Technology, Institut Teknologi Bandung, Jalan Ganesha No. 10 Bandung 40132, Indonesia; e: Department of Forest Production, Faculty of Forestry, Universiti Putra Malaysia, 43400 UPM, Serdang, Selangor D.E., Malaysia; \* Corresponding author: akhalilhps@gmail.com (H.P.S Abdul Khalil)

### INTRODUCTION

The importance of the acid hydrolysis of lignocellulosic fibers is derived from its ability to isolate micron-sized cellulose particles known as microcrystalline cellulose (MCC) as well as nanocrystalline cellulose (NCC), which can be used as a green and environmentally friendly bio-filler for various applications in the medical, food, cosmetics, and packaging industries (Abdul Khalil *et al.* 2014). The acid hydrolysis of cellulose is a complex heterogeneous reaction comprised of the formation of a conjugated acid, the scission of the C-O bond, and finally the liberation of short chains (Wyman *et al.* 2005). In this procedure, the reaction of glucan and water is catalyzed by an acid (Li and Zhao 2007). The aim of acid hydrolysis is the removal of the amorphous part (hemicellulose and disordered regions of cellulose), which leaves the crystalline section unchanged and reduces the size of the fibers. Acid causes the scission of hemicellulose to xylose and then xylose to furfural (Adel *et al.* 2010). The removal of cementing regions of the fibers through acid hydrolysis boosts their crystallinity (Safinas *et al.* 2013). Acid hydrolysis can be performed using formic acid (Sun *et al.* 2008), phosphoric acid (H<sub>3</sub>PO<sub>4</sub>) (Hong *et al.* 2012), nitric acid (HNO<sub>3</sub>) (Horst *et al.* 2010), hydrochloric acid (HCl) (Kumar *et al.* 2013), and sulfuric acid (H<sub>2</sub>SO<sub>4</sub>) (Ohwoavworhwa *et al.* 2009; Vanhatalo and Dahl 2014). However, HCl and H<sub>2</sub>SO<sub>4</sub> are the most commonly used acids in the acid hydrolysis process.

Because both HCl and H<sub>2</sub>SO<sub>4</sub> have a high acid dissociation constant (a quantitative indicator used to measure the power of an acid in solution), they possess a superior ability to hydrolyze  $\beta$ -1,4-glucosidic bonds (Zaini *et al.* 2013). In contrast to hydrolysis by HCl, hydrolysis by H<sub>2</sub>SO<sub>4</sub> modifies the surface of the cellulose become a negatively charged surface, resulting from the esterification of hydroxyl groups by sulphate ions (Haafiz *et al.* 2014). However, H<sub>2</sub>SO<sub>4</sub> hydrolysis suffers from low thermal stability because of the sulfate groups on the surface of fibers, which causes a dehydration reaction (Fahma *et al.* 2011). Therefore, a neutralization step using NaOH usually increases the thermal stability of H<sub>2</sub>SO<sub>4</sub>-hydrolyzed fibers (Kargarzadeh *et al.* 2012).

Hydrolysis conditions, such as reaction time, temperature, and acid concentration, affect the properties of the hydrolyzed fibers. It has been proposed that to obtain significant hydrolysis at low acid concentrations, greater temperature and, therefore, energy, is needed (Horst *et al.* 2010). As stated by Beck-Candanedo *et al.* (2005) and Rojas *et al.* (2011), acid concentration and reaction time are two important parameters in the acid hydrolysis process. The importance of time in the acid hydrolysis process is derived from the individual rate of hydrolytic attack at its three different stages, where the initial stage is a rapid hydrolytic attack of acid on the more accessible amorphous segments and the latter stage is a much slower hydrolytic attack to the amorphous parts and/or at crystal surfaces (Foston *et al.* 2011). It has been reported that acid hydrolysis reduces the degree of polymerization (DP) exponentially as a function of time and the rate of acid hydrolysis (Thoorens *et al.* 2014). Because a hydrolysis reaction time that is too long leads to the complete digestion of cellulosic fibers to sugar and a reaction time that is too short produces just aggregates (Beck-Candanedo *et al.* 2005), selecting an appropriate hydrolysis time is a crucial step in the acid hydrolysis of cellulosic fibers. Increasing the hydrolysis time, promoting longer contact of the acid with fibers, has a great effect on the cellulose because of the sensitivity of the  $\beta$ -1,4-glycosidic bond to acid (Adel *et al.* 2010). Therefore, the proper conditions of acid hydrolysis impact both the efficient removal of hemicellulose and the degradation of cellulose (Foston *et al.* 2011).

The effect of hydrolysis duration on the properties of various fibers has been investigated (El-Sakhawy and Hassan 2007; Das *et al.* 2010; Adel *et al.* 2011; Foston *et al.* 2011; Rojas *et al.* 2011; Vanhatalo and Dahl 2014). Kenaf has gained researchers' attention as a non-wood cellulosic source to produce MCC (Keshk and Haija 2011; Safinas *et al.* 2013; Wang *et al.* 2013) and NCC (Kargarzadeh *et al.* 2012; Zaini *et al.* 2013), because of its high cellulose content (approximately 55%), and mechanical characteristics (Abdul Khalil *et al.* 2010; Khalil and Suraya 2011). For example, Wang and Cheng (2009) compared the effect of 5% HCl hydrolysis on the properties of kenaf bast, core, and wood fibers, while Keshk and Haija (2011) studied the impact of various HCl concentrations on the properties of kenaf bast and BC. The hydrolysis of kenaf bast, when using 2 M HCl as a filler over the course of 3 h, was performed by Safinas *et al.* (2013), and a comparison between the HCl and H<sub>2</sub>SO<sub>4</sub> hydrolysis of kenaf bast was studied by Zaini *et al.* (2013). Kargarzadeh *et al.* (2012) evaluated the influence of H<sub>2</sub>SO<sub>4</sub> hydrolysis time (20 to 120 min) on the properties of kenaf bast NCC.

Although the hydrolysis of HCl for the production of MCC from kenaf bast has been reported, limited studies have been dedicated to exploring the influence of hydrolysis duration, which is one of the vital parameters affecting the properties of hydrolyzed kenaf bast.

Therefore, the primary objective of this research was to isolate MCC from kenaf bast by means of hydrolysis by HCl conducted for various reaction times. Furthermore, the characteristics of MCC were analyzed regarding yield, morphology, functional group, crystallinity, crystallite size, particle size, and thermal properties.

## EXPERIMENTAL

### Materials

The kenaf bast fibers were obtained from the National Kenaf and Tobacco Board, Malaysia. Analytical-grade hydrochloric acid (HCl) (37%) was supplied by OReC (Asia). Bleached kenaf pulps were prepared based on a previously described technique (Davoudpour and Abdul Khalil 2013).

### MCC Preparation

Approximately 10 g of the bleached kenaf bast fibers was hydrolyzed using 1.5 M HCl at 80 °C for 1, 2, or 3 h. The ratio of acid to kenaf fiber was kept constant at 20:1. The hydrolysis process was carried out in a water bath. Upon completion of the reaction, the fibers were washed and rinsed with distilled water through a membrane filter (Nyla membrane disc filter, 0.2 µm, Pall Corporation, Malaysia) until it reached pH 7. Subsequently, the obtained MCC were dried in an oven at 60 °C for 24 h. Finally, the MCC were stored in a desiccator until further analysis. The yields of MCC were calculated based on the oven-dried weight of the fibers.

### Characterization

#### *Morphology*

The morphological studies of the samples were carried out by means of scanning electron microscopy (SEM, model: EVO MA10, Carl-ZEISS, Germany). The acid-hydrolyzed samples were gold coated using Polaron (Fisons) SC515 Sputter coater (VG, Micrtech, Sussex, UK), and analysis was performed using an acceleration voltage of 15 kV. The length and diameter of the fibers were measured using image analyzer software (Image Pro Plus Version 7.01, Media Cybernetics, Inc., USA) and reported as the mean value of 100 measurements.

#### *Functional group analysis*

The functional groups of the kenaf bast MCC produced at various hydrolysis times were analyzed using Fourier transform infrared spectroscopy (FT-IR) (Nicolet iS 10 FT-IR Spectrometer, Thermo Scientific, United States). First, the samples were ground and dried in an oven for 24 h at 60 °C. Approximately 7 mg of each sample was mixed with KBr to obtain a total of 100 mg. The KBr was used to hold the flour in place during the test. Transparent pellets were prepared and analyzed in the wavelength range of 400 to 4000 cm<sup>-1</sup>.

#### *Crystallinity and crystal size determination*

The crystallinity of the acid-hydrolyzed kenaf bast fibers was determined using an X-ray diffraction (XRD) (model: D8 Advanced Bruker, Germany) at an operating voltage of 40 kV. The applied current was 44 mA. The crystallinity of the samples was calculated using Eq. 1 (Segal formula) between the angles 10° and 30° of 2θ,

$$CrI(\%) = \frac{I_{200} - I_{AM}}{I_{200}} \times 100 \quad (1)$$

where  $I_{200}$  symbolizes the amorphous and crystalline fractions and  $I_{AM}$  denotes the amorphous region (Shi *et al.* 2011)

The crystal size of samples was estimated based on the Scherrer equation (Eq. 2) for the 002 lattice plane of the fibers:

$$D_{(hkl)} = \frac{K\lambda}{\beta_0 \cos\theta} \quad (2)$$

where  $D_{(hkl)}$  is the crystal size (nm),  $K$  is the Scherrer constant,  $\lambda$  is the wavelength of XRD,  $\beta_0$  is the full width at half-maximum of the reflection, and  $\theta$  is the Bragg angle.

#### Particle size

The particle size and size distribution analyses were performed using a Master-sizer 2000 Version 5.60 particle size analyzer (Malvern Instruments Ltd., Malvern, UK). The mean particle diameter of each sample was reported as the average value of three replicates.

#### Thermogravimetric analysis (TGA)

A TGA/SDTA 851 (Mettler Toledo, Switzerland) was applied to investigate the thermal stability of the samples. Approximately 3 to 6 mg of the acid-hydrolyzed fibers was heated from 25 to 550 °C in a nitrogen atmosphere at a heating rate of 20 °C/min. The DTG and TGA curves are reported as the results of this analysis for three replications.

## RESULTS AND DISCUSSION

### Yield

In this study, kenaf bast MCC was produced using three different acid hydrolysis times (1, 2, and 3 h) while maintaining a constant HCl concentration, temperature, and acid-to-fiber ratio. The obtained yields of kenaf bast MCC as a function of reaction time are tabulated in Table 1 as an average of three replicates. The yields of the one-hour, two-hour, and three-hour hydrolyzed kenaf bast MCC were found to be  $84.7 \pm 1.2\%$ ,  $82.8 \pm 1.2\%$ , and  $80.9 \pm 1.1\%$ , respectively.

Reduction of the yield of resultant kenaf bast MCC by increasing the hydrolysis duration is probably due to the break-down of the more  $\beta$ -1,4 glycosidic bond at higher reaction time and easier removal of short chains during hydrolysis. A similar trend was observed by Vanhatalo and Dahl (2014). Adel *et al.* (2011) observed that there was an optimum reaction time for the hydrolysis of rice and bean hulls using 2% HCl at 120 °C, such that at longer hydrolysis times, the yield decreased.

The range of yields in this study was similar to the yields of kenaf bast MCC (80%) as reported by Wang *et al.* (2012), who used the same HCl concentration for 1 h at a higher temperature (105 °C). Also, the yields were greater than the maximum yield of kenaf bast MCC (66%) reported by Keshk and Haija (2011). The yield of kenaf bast MCC in this study was also higher than the yield from rice hulls and bean hulls (77.58% and 73.84%, respectively) (Adel *et al.* 2011) and the yield from sawdust (68%) (Oyeniya and Itiola

2012), and slightly lower than the yield from rice straw (94.6%) (Ilindra and Dhake 2008) when prepared by HCl hydrolysis.

### Morphological Analysis

The morphological structure of kenaf bast MCC was studied using SEM, as shown in Fig. 1. The morphology of all samples was rod-like. Wang *et al.* (2012) compared this rod-like structure of kenaf bast MCC to non-porous glass fibers. The diameters of the HCl-hydrolyzed fibers were found to be  $10.05 \pm 1.51 \mu\text{m}$ ,  $8.89 \pm 1.28 \mu\text{m}$  and  $7.9 \pm 1.13 \mu\text{m}$  at 1, 2, and 3 h, respectively. As can be seen, the diameter of the kenaf bast MCC decreased with increasing hydrolysis time. In contrast to its effect on the bleached fibers (diameter of  $10.98 \mu\text{m}$ ), HCl hydrolysis conducted for 1 h did not greatly change the diameter of the kenaf bast MCC. This could be ascribed to the mild hydrolysis conditions and probably the low amount of hemicellulose remaining after bleaching. Shi *et al.* (2011) also reported minimal changes in the diameter of acid-hydrolyzed kenaf bast fibers ( $9.58 \mu\text{m}$ ) after bleaching ( $10.63 \mu\text{m}$ ). The decrease in the diameter of kenaf bast MCC observed in this study was more likely due to the removal of the more amorphous regions, *e.g.*, the hemicelluloses that surrounded the microfibrils.

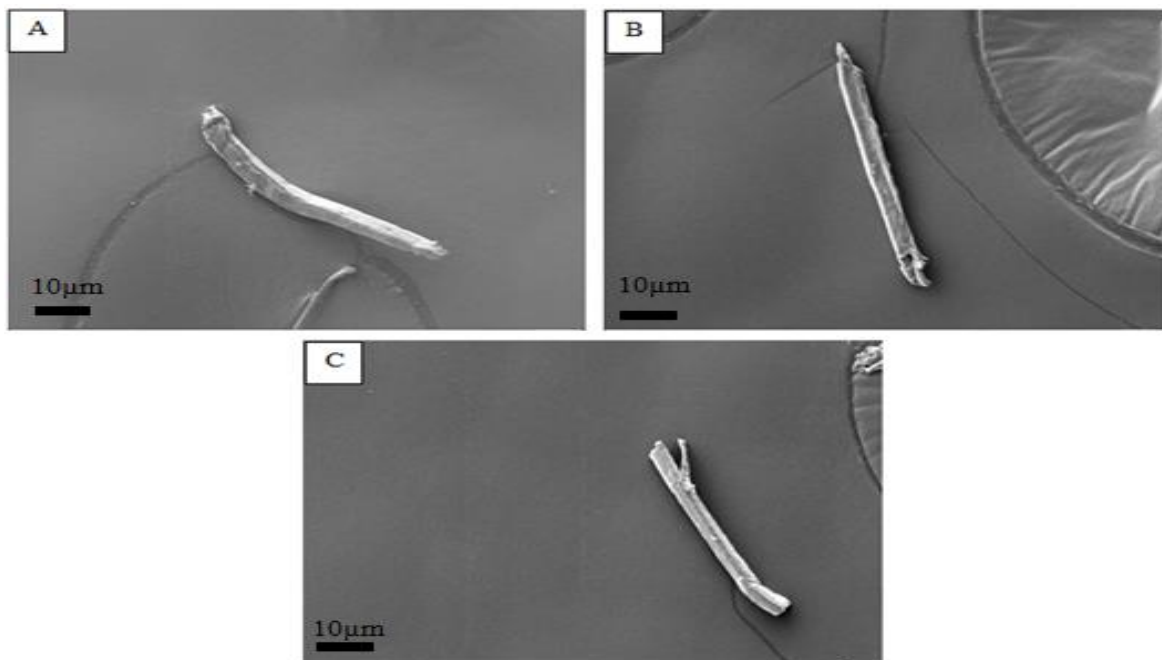


**Fig. 1.** SEM micrographs of representative kenaf bast MCC subjected to hydrolysis for (A) 1 h, (B) 2 h, and (C) 3 h

Meanwhile, the less-obvious changes in the diameter were probably attributable to the small amount of remaining hemicellulose. Basically, in the early stages of hydrolysis, acid diffuses favorably into the amorphous portions of cellulosic fibers and hydrolyzes the glycosidic bonds that are easily accessible. The further progression of the reaction at the reducing end and on the surface of the remaining crystalline regions occurs much more slowly (Dong *et al.* 1998). In other words, low-molecular weight cellulose can be produced as follows: first, the non-crystalline parts of the cellulose are hydrolyzed, until only dense cellulose with approximately 80% crystallinity remains. Subsequently, the substantial parts of the cellulose can be hydrolyzed with higher acid concentrations and longer

hydrolysis time (Nada *et al.* 2009). However, the less-obvious changes in the diameter of fibers, caused by increasing the duration of the hydrolysis reaction, could be due to the slow rate of the reaction in the crystalline regions of fibers and the relatively stable dimensions of the fibers. The length of kenaf bast MCC was reduced noticeably with increasing hydrolysis time, from  $150 \pm 19 \mu\text{m}$  (1h) to  $100 \pm 12 \mu\text{m}$  (3h). The noteworthy reduction in the length of kenaf bast MCC with the increase in reaction time probably occurred because of the damaging effect of the acid at the intermediate positions of the long chains, breaking down the glycosidic bonds and releasing the shorter-chained oligomers (Nada *et al.* 2009; Mandal and Chakrabarty 2011). As Mandal and Chakrabarty (2011) reported, the formation of short-length crystals is related to the hydrolysis of the pyranose linkages during the acid hydrolysis process.

### Fourier Transform Infrared Spectroscopy (FT-IR)

The FT-IR spectra of the HCl-hydrolyzed MCC subject to acid hydrolysis times are depicted in Fig. 2. As can be seen in this figure, all spectra are similar, which indicates similarity in the chemical compositions of all samples. Similar results were achieved by Keshk and Haija (2011) when they compared MCC from kenaf bast to MCC from bacterial cellulose. Moreover, Zaini *et al.* (2013) reported the same results during the isolation of NCC from kenaf bast using 2.5 M HCl at 105 °C for 20 min.

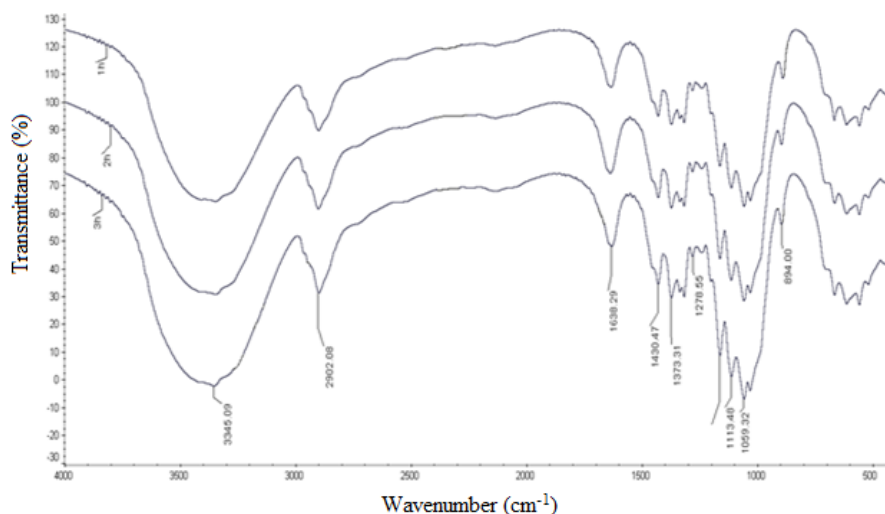


**Fig. 2.** FT-IR spectra of kenaf bast MCC after 1, 2, and 3 h of hydrolysis

The absorption peaks found at 3300 to 3500  $\text{cm}^{-1}$  and at 2900  $\text{cm}^{-1}$  were attributed to the hydrogen bond (OH groups stretching) and CH groups, respectively (Adel *et al.* 2011; Azubuike and Okhamafe 2012). It is evident from this figure that by increasing the hydrolysis time, the intensity of the hydrogen bonds increased. This might have been because of the degradation of the amorphous part, which enhanced the crystallinity of the MCC as time progressed. Furthermore, the OH band shifted to lower wavenumbers with increasing hydrolysis time, which can be ascribed to the increased hydrogen bonding and crystallinity of the MCC. Nada *et al.* (2009) reached a similar conclusion: by increasing the acid concentration, the hydrogen bond of raw cotton linter (at 3419  $\text{cm}^{-1}$ ) would shift to a lower wave number (3340  $\text{cm}^{-1}$ ) because of the increase in the OH bond in the cotton linter chains. The absorption band at 1640  $\text{cm}^{-1}$  in all three samples was due to water

absorption (Chan *et al.* 2012; Haafiz *et al.* 2013). The peaks at 1430 and 1373  $\text{cm}^{-1}$  were assigned to  $\text{CH}_2$  and CH bending vibration, respectively (Nazir *et al.* 2013; Pachuau *et al.* 2013). The absorption band at 1163  $\text{cm}^{-1}$  is indicative of an ether linkage (Chan *et al.* 2012; Haafiz *et al.* 2013). The absence of absorption bands at 1242, 1500, and 1700  $\text{cm}^{-1}$ , which can be attributed to lignin and hemicellulose, confirmed the elimination of these two components (Haafiz *et al.* 2013; Nazir *et al.* 2013). Additionally, the peak at 894  $\text{cm}^{-1}$  was attributed to anti-symmetric out-of-plane OH stretching resulting from the  $\beta$ -linkage (Adel *et al.* 2011; Keshk and Haija 2011).

The FT-IR peaks in this study were similar to those in the MCC spectra obtained from other cellulosic sources (Adel *et al.* 2011; Keshk and Haija 2011; Azubuike and Okhamafe 2012; Haafiz *et al.* 2013; Nazir *et al.* 2013; Pachuau *et al.* 2013). Furthermore, the FT-IR analysis found no changes in the chemical components of kenaf bast MCC as a result of increased hydrolysis time; the only changes observed were alternations in the intensity and/or wavenumber of some peaks. In comparison with the bleached fibers, no alteration in the chemical compositions of the acid-hydrolyzed MCC was observed. Although the acid hydrolysis had an effect on the crystallinity and morphology of the fibers, it did not influence the chemical components of the fibers.

### X-Ray Diffraction (XRD)

Because the higher crystallinity of the acid-hydrolyzed MCC led to a higher tensile strength of the fibers due to the increased rigidity of the cellulose (Haafiz *et al.* 2013), studying the crystallinity can be used as a means to provide necessary information about this issue. The XRD diffractograms of 1-, 2-, and 3-h acid-hydrolyzed MCC are illustrated in Fig. 3. Additionally, the crystallinity percentage and crystal size, as measured by Eqs. 1 and 2, respectively, are summarized in Table 1. The diffraction patterns of all samples were similar and resembled native cellulose with  $2\theta$  degrees at  $18^\circ$  and  $22.5^\circ$ .

The crystallinity values of the samples were  $81.3 \pm 1.4\%$ ,  $82.7 \pm 1.2\%$ , and  $82 \pm 1.3\%$  after 1, 2, and 3 h, respectively. Moreover, in comparison with bleached fibers (crystallinity of 72%), the kenaf bast MCC showed obviously higher crystallinity, probably because of the elimination of amorphous regions, the cleavage of glycosidic bonds, and the subsequent release of more individual crystals. As can be seen in Table 1, a slight increase (around 1.62%) in the crystallinity of the MCC was observed when the reaction time was increased from 1 to 2 h.

When the amorphous regions that hold the crystalline parts dissolve during acid hydrolysis, single crystals are released and the crystallinity increases. In other words, by eliminating the cementitious materials using acid hydrolysis, cellulose chains can become better packed (Safinas *et al.* 2013). Therefore, high crystallinity can be translated as ordered and dense molecular structures (Azubuike and Okhamafe 2012). Besides, increasing crystallinity measure by Segal method here can be attributed to increasing the crystal size (French and Cintrón 2013). A further increase in the reaction time to 3 h caused an approximately 0.81% reduction in the crystallinity value, probably because of damage to the MCC crystalline regions during the longer hydrolysis duration. Vanhatalo and Dahl (2014) reported the same observations and explanations. It is believed that after hydrolysis of accessible glycosidic bonds, further reactions at the reducing end and the surface of the remaining crystalline regions occurs much more slowly (Dong *et al.* 1998). Thus, the very small reduction in the crystallinity of MCC observed with the increase from 2 to 3 h might be due to very moderate damage to some of the crystalline sections. These data are in agreement with the findings of Kargarzadeh *et al.* (2012), who found that by increasing the

hydrolysis time to 40 min, the crystallinity of kenaf bast NCC increased from 75.1% to 81.8%, and at longer times, it decreased to 75.3%. This was attributed to the partial destruction of the crystalline parts of NCC because of the high concentration of H<sub>2</sub>SO<sub>4</sub>.

**Table 1.** Yield, Crystallinity, and Crystal Size Data for Kenaf Bast MCC

Samples	Yield (%)	Cr (%)	Crystalline size (nm)
1 h	84.7 ±1.2	81.3±1.4	6.23±0.21
2 h	82.8±1.2	82.7±1.2	6.43±0.12
3 h	80.9±1.1	82.0±1.3	6.76±0.24

The crystallinity percentages obtained in this study were in the range of those from other literature on MCC (Nada *et al.* 2009; Azubuiké and Okhamafe 2012; Chauhan and Chakrabarti 2012; Haafiz *et al.* 2013) and higher than that found by Wang *et al.* (2012) using the same HCl concentration (77.7%). This was perhaps due to the longer hydrolysis time at a lower temperature in this study, which broke down more glycosidic bonds (in the amorphous regions) and further increased the crystallinity. The crystal sizes were found to be 6.23, 6.43, and 6.76 nm at 1, 2, and 3 h, respectively. From the data, a slight increase in the crystallite size of kenaf bast MCC in concert with the increase in hydrolysis time was observed. An increase in the crystallite size of MCC was also described by Das *et al.* (2010). They explained that the loose structure of the celluloses favored alteration in the crystal size and that the degradation of smaller crystals as well as the growth of defective crystals was responsible for increasing the crystallite size. By increasing hydrolysis time, with the removal of more lignin and hemicellulose and leaving behind the dense cellulose, the density fluctuation increased. This was because of lateral coalescence of microfibrils and their co-crystallization, leading to increased apparent crystal size (Nishiyama *et al.* 2014). In addition, smaller crystal size formation at 1 h can be attributed to higher surface area in the fiber and hence greater accessibility to chemicals (Reddy and Yang 2005) and higher chain loss per crystal. SEM micrographs showed a larger crystal size that might be attributed to the preparation process of samples for XRD and crystal size analysis in powder form compared to sample preparation in SEM analysis.

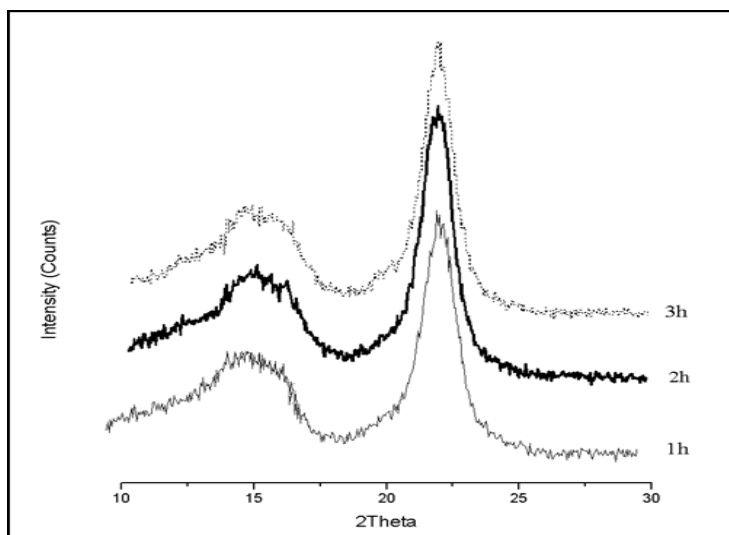


**Fig. 3.** XRD diffractograms of kenaf bast MCC

## Particle Size Analysis

The determination of particle size and its distribution is an important issue for the final application of MCC. These criteria depend on many different parameters, such as the structure of the sample, acid concentration, hydrolysis time, and temperature (Das *et al.* 2010; Wang *et al.* 2010). However, after the drying of MCC, the particle size distributions of the powders depend on the extent of their aggregation (Das *et al.* 2010). The results of the particle size analysis of kenaf bast MCC at various hydrolysis times are tabulated in Table 2.

**Table 2.** Particle Size Analysis of Kenaf Bast MCC

Samples	$D(v, 0.1)$ ( $\mu\text{m}$ )	$D(v, 0.5)$ ( $\mu\text{m}$ )	$D(v, 0.9)$ ( $\mu\text{m}$ )
1 h	15.53±0.46	73.36±1.02	386.35±4.21
2 h	14.61±0.28	66.40±1.53	288.25±3.75
3 h	14.17±0.34	66.25±1.15	256.85±4.02

The particle size was reported based on volume percentage.  $D(v, 0.1)$  shows that 10% of MCC are smaller than this diameter;  $D(v, 0.5)$  indicates that 50% of MCC are larger than this diameter and 50% are smaller than this diameter; finally,  $D(v, 0.9)$  points out that 90% of MCC are smaller than this diameter. Also,  $D(v, 0.5)$  expresses the median diameter of kenaf bast MCC. The range of particle sizes for all samples was between 4 and 550  $\mu\text{m}$ . This range of MCC sizes was in agreement with the range reported by Wang *et al.* (2010) for kenaf bast MCC. The median particle sizes of the hydrolyzed MCC at 1, 2, and 3 h were found to be 73.3, 66.4, and 66.2  $\mu\text{m}$ , respectively. As seen from this table, by increasing the reaction time, the median particle size was reduced, though this reduction was not remarkable after 2 h. This can be attributed to the slightly greater crystal size of MCC at 3 h compared with 2 h, which caused a reduction in the breakdown of the crystal structure (Das *et al.* 2010).

## TGA Analysis

The influence of hydrolysis time on the thermal stability of the acid-hydrolyzed MCC was evaluated by means of TGA analysis. Figure 4 displays the TGA and DTG curves of the kenaf bast MCC. Furthermore, the thermal characteristics of the samples, *i.e.*,  $T_{\text{onset}}$  (initial degradation temperature),  $T_{\text{max}}$  (maximum degradation temperature), and char residue, are summarized in Table 3.

**Table 3.** Thermal Characteristics of Kenaf Bast MCC

Samples	$T_{\text{onset}}$ ( $^{\circ}\text{C}$ )	$T_{\text{max}}$ ( $^{\circ}\text{C}$ )	Residue at 550 $^{\circ}\text{C}$ (%)
1 h	321±2.43	362±2.51	12±0.51
2 h	317±2.18	358±2.32	11±0.23
3 h	314±2.13	355±2.26	10±0.16

According to the TGA curves, all samples showed similar decomposition patterns (two decomposition steps), with an initial mass loss of around 6% between 25 and 150  $^{\circ}\text{C}$ . This weight loss was attributed to the evaporation of water. As can be observed from the table, the  $T_{\text{onset}}$  values of 1-, 2-, and 3-h kenaf bast MCC were 321, 317, and 314  $^{\circ}\text{C}$ , respectively. The results illustrate that with increasing reaction time, the MCC began to degrade at a lower temperatures, and the thermal stability therefore declined.

Furthermore, the maximum degradation temperature ( $T_{\max}$  obtained from DTG thermograms) of the samples occurred at 362, 358, and 355 °C for 1 h, 2 h, and 3 h treated kenaf bast MCC, respectively.  $T_{\max}$  was ascribed to the decomposition of cellulose. In comparison with bleached kenaf bast fibers,  $T_{\max}$  was reduced from 368 °C to 355 to 362 °C. This might have been due to the creation of short and free end-chain particles that could be degraded at lower temperatures (Wang *et al.* 2007). Similar results were proposed by Haafiz *et al.* (2013). In other words, by increasing the hydrolysis duration from 1 to 3 h, thermal stability decreased, perhaps because of some destruction of the crystalline parts of the fibers over the longer reaction time.

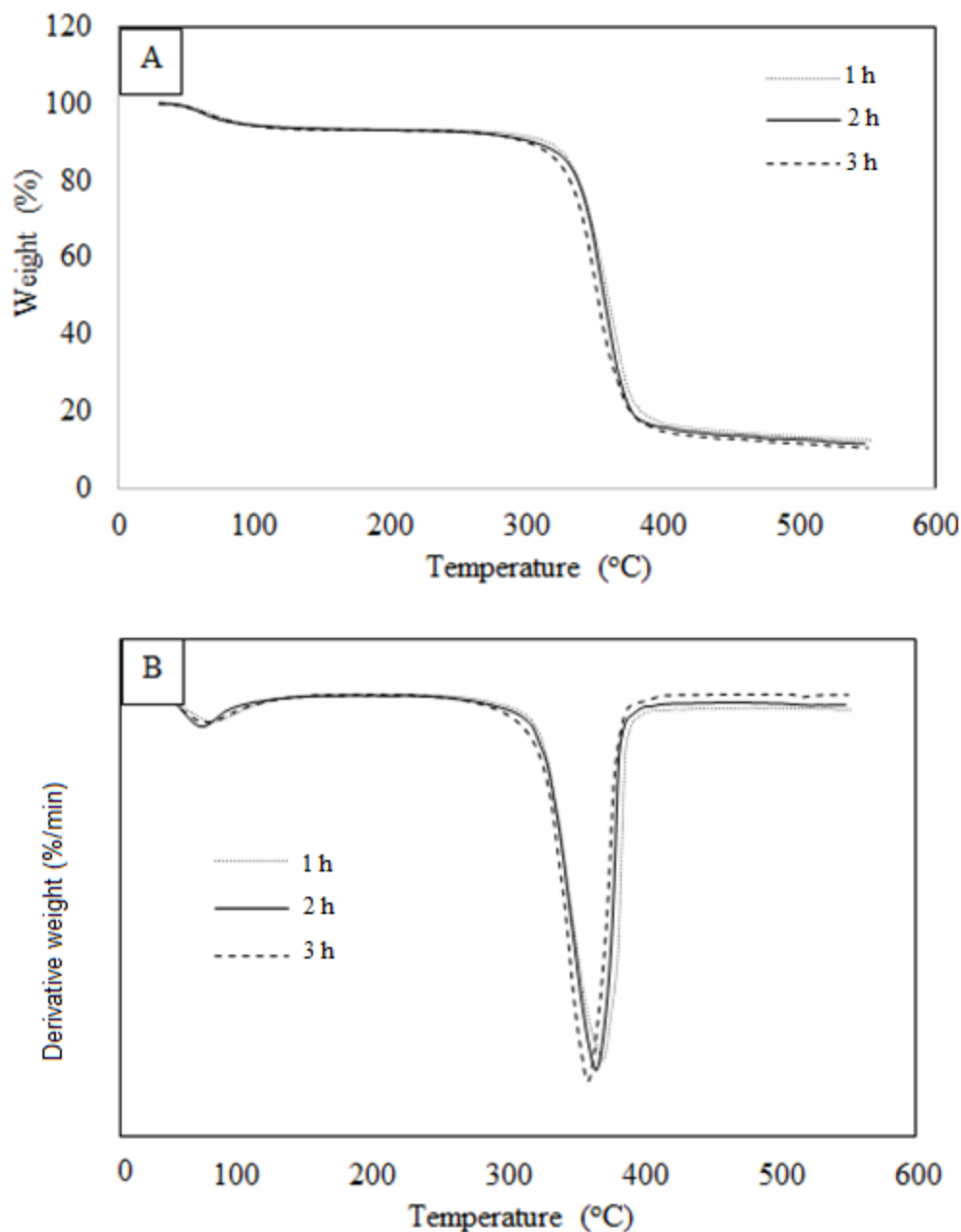


Fig. 4. (A) TGA and (B) DTG of kenaf bast MCC

Kargarzadeh *et al.* (2012) also proposed that with increasing hydrolysis time of kenaf bast fibers, the thermal stability of NCC was reduced. They ascribed these results to the low molecular weight of the fibers formed during the hydrolysis as well as to the long interaction time between H<sub>2</sub>SO<sub>4</sub> and kenaf, which can form more sulfate groups and diminish thermal stability. However, the maximum degradation temperature of HCl-treated fibers in this study was higher than that of OPEFB-MCC (326 °C) (Haafiz *et al.* 2013), cotton linter-MCC (320 °C) (Nada *et al.* 2009), and kenaf bast nanofibers (320 °C) (Jonoobi *et al.* 2009), but close to that of kenaf bast NCC (358 °C) (Zaini *et al.* 2013).

Char can be defined as non-volatile carbonaceous components that are generated by pyrolysis (Azubuike and Okhamafe 2012). As can be seen in Table 3, when the reaction time increased, the amount of char residue from the kenaf bast MCC decreased. These results are in agreement with the findings of Azubuike and Okhamafe (2012), who reported a reduction in char formation of MCC from corncob as a result of increasing hydrolysis time. Moreover, the amount of char in the MCC (10% to 12%) was slightly lower than that in bleached fibers (13%), probably because of the removal of more hemicelluloses during the HCl hydrolysis.

## CONCLUSIONS

1. It was observed that an increase in hydrolysis time decreased particle size, including both the diameter and length of microcrystalline cellulose (MCC).
2. The yields of the HCl-hydrolyzed kenaf bast MCC were found to be decreased from 84.7±1.2% to 80.9±1.1% with increasing hydrolysis time of 1h to 3h.
3. The diameters of the HCl-hydrolyzed fibers were found to be 10.05 µm, 8.89 µm, and 7.9 µm at 1 h, 2 h, and 3 h hydrolysis time, respectively. The length of kenaf bast MCC reduced with acid hydrolysis time from 150 µm (1 h) to 100 µm (3 h).
4. The FT-IR analyses revealed that the acid hydrolysis had an effect on the crystallinity the fibers; however it did not influence the chemical components of the fibers.
5. The crystallinity values of MCC fiber gradually increased from 1 h (81.3±1.4%) to 2 h (82.7±1.2%), and they decreased thereafter (82±1.3%).
6. The thermal analyses of MCC kenaf bast fiber showed the  $T_{\text{onset}}$  values of 321 °C, 317 °C, and 314 °C; the maximum degradation temperatures were 362 °C, 358 °C, and 355 °C for acid hydrolysis times of 1 h, 2 h, and 3 h, respectively.

## ACKNOWLEDGEMENTS

The research was supported by the Universiti Sains Malaysia (USM), Penang, Malaysia under Research Grant no. RUI-1001/PTEKIND/814255.

## REFERENCES CITED

- Abdul Khalil, H., Davoudpour, Y., Islam, M. N., Mustapha, A., Sudesh, K., Dungani, R., and Jawaid, M. (2014). "Production and modification of nano-fibrillated cellulose using various mechanical processes: A review," *Carbohydrate Polymers* 99, 649-665. DOI: 10.1016/j.carbpol.2013.08.069
- Abdul Khalil, H., Yusra, A., Bhat, A., and Jawaid, M. (2010). "Cell wall ultrastructure, anatomy, lignin distribution, and chemical composition of Malaysian cultivated kenaf fiber," *Industrial Crops and Products* 31(1), 113-121. DOI: 10.1016/j.indcrop.2009.09.008
- Adel, A. M., El-Wabah, Z. H. A., Ibrahim, A. A., and Al-Shemy, M. T. (2010). "Characterization of microcrystalline cellulose prepared from lignocellulosic materials. Part I. Acid catalyzed hydrolysis," *Bioresource Technology* 101(12), 4446-4455. DOI:10.1016/j.biortech.2010.01.047
- Adel, A. M., El-Wabah, Z. H. A., Ibrahim, A. A., and Al-Shemy, M. T. (2011). "Characterization of microcrystalline cellulose prepared from lignocellulosic materials. Part II: Physicochemical properties," *Carbohydrate Polymers* 83(2), 676-687. DOI: 10.1016/j.carbpol.2010.08.039
- Azubuiké, C. P., and Okhamafe, A. O. (2012). "Physicochemical, spectroscopic and thermal properties of microcrystalline cellulose derived from corn cobs," *International Journal of Recycling of Organic Waste in Agriculture* 1, 1-7. DOI: 10.1186/2251-7715-1-9
- Beck-Candanedo, S., Roman, M., and Gray, D. G. (2005). "Effect of reaction conditions on the properties and behavior of wood cellulose nanocrystal suspensions," *Biomacromolecules* 6(2), 1048-1054. DOI: 10.1021/bm049300p
- Chauhan, V. S., and Chakrabarti, S. K. (2012). "Use of nanotechnology for high performance cellulosic and papermaking products," *Cellulose Chemistry and Technology* 46(5-6), 389-400. DOI: 10.1021/bm049300p
- Das, K., Ray, D., Bandyopadhyay, N., Gupta, A., Sengupta, S., Sahoo, S., Mohanty, A., and Misra, M. (2010). "Preparation and characterization of cross-linked starch/poly (vinyl alcohol) green films with low moisture absorption," *Industrial and Engineering Chemistry Research* 49(5), 2176-2185. DOI:10.1021/ie901092n
- Davoudpour, Y., and Abdul Khalil, H. P. S. (2013). "Innovating biofibers for sustainable future," *2nd International Conference on Kenaf and Allied Fibres (ICKAF 2013)*, Universiti Putra Malaysia, Kuala Lumpur, Malaysia.
- Dong, X. M., Revol, J.-F., and Gray, D. G. (1998). "Effect of microcrystallite preparation conditions on the formation of colloid crystals of cellulose," *Cellulose* 5(1), 19-32. DOI:10.1023/A:1009260511939
- El-Sakhawy, M., and Hassan, M. L. (2007). "Physical and mechanical properties of microcrystalline cellulose prepared from agricultural residues," *Carbohydrate Polymers* 67(1), 1-10. DOI:10.1016/j.carbpol.2006.04.009
- Fahma, F., Iwamoto, S., Hori, N., Iwata, T., and Takemura, A. (2011). "Effect of pre-acid-hydrolysis treatment on morphology and properties of cellulose nanowhiskers from coconut husk," *Cellulose* 18(2), 443-450. DOI:10.1007/s10570-010-9480-0
- Foston, M. B., Hubbell, C. A., and Ragauskas, A. J. (2011). "Cellulose isolation methodology for NMR analysis of cellulose ultrastructure," *Materials* 4(11), 1985-2002. DOI: 10.3390/ma4111985

- French, A. D., and Cintron, M. S. (2013). "Cellulose polymorphy, crystallite size, and the Segal crystallinity index," *Cellulose* 20, 583-588. DOI 10.1007/s10570-012-9833-y
- Haafiz, M.K.M., Eichhorn, S., Hassan, A., and Jawaid, M. (2013). "Isolation and characterization of microcrystalline cellulose from oil palm biomass residue," *Carbohydrate Polymers* 93(2), 628-634. DOI:10.1016/j.carbpol.2013.01.035
- Haafiz, M. K. M., Hassan, A., Zakaria, Z., and Inuwa, I. M. (2014). "Isolation and characterization of cellulose nanowhiskers from oilpalm biomass microcrystalline cellulose," *Carbohydrate Polymers* 103, 119-125. DOI: 10.1016/j.carbpol.2013.11.055
- Hong, B., Xue, G., Weng, L., and Guo, X. (2012). "Pretreatment of moso bamboo with dilute phosphoric acid," *BioResources* 7(4), 4902-4913. DOI: 10.15376/biores.7.4.4902-4913
- Horst, W. J., Wang, Y., and Eticha, D. (2010). "The role of the root apoplast in aluminium-induced inhibition of root elongation and in aluminium resistance of plants: A review," *Annals of Botany* 106(1), 185-197. DOI:10.1093/aob/mcq053
- Iindra, A., and Dhake, J. (2008). "Microcrystalline cellulose from bagasse and rice straw," *Indian Journal of Chemical Technology* 15, 497-499.
- Jonoobi, M., Niska, K. O., Harun, J., and Misra, M. (2009). "Chemical composition, crystallinity, and thermal degradation of bleached and unbleached kenaf bast (*Hibiscus cannabinus*) pulp and nanofibers," *BioResources* 4(2), 626-639. DOI: 10.15376/biores.4.2.626-639
- Kargarzadeh, H., Ahmad, I., Abdullah, I., Dufresne, A., Zainudin, S. Y., and Sheltami, R. M. (2012). "Effects of hydrolysis conditions on the morphology, crystallinity, and thermal stability of cellulose nanocrystals extracted from kenaf bast fibers," *Cellulose* 19(3), 855-866. DOI:10.1007/s10570-012-9684-6
- Keshk, S. M., and Haija, M. A. (2011). "A new method for producing microcrystalline cellulose from *Gluconacetobacter xylinus* and kenaf," *Carbohydrate Polymers* 84(4), 1301-1305. DOI:10.1016/j.carbpol.2011.01.024
- Khalil, H. A., and Suraya, N. L. (2011). "Anhydride modification of cultivated kenaf bast fibers: Morphological, spectroscopic and thermal studies," *BioResources* 6(2), 1122-1135. DOI: 10.15376/biores.6.2.1122-1135
- Kumar, R., Hu, F., Hubbell, C. A., Ragauskas, A. J., and Wyman, C. E. (2013). "Comparison of laboratory delignification methods, their selectivity, and impacts on physiochemical characteristics of cellulosic biomass," *Bioresource Technology* 130, 372-381. DOI:10.1016/j.biortech.2012.12.028
- Li, C., and Zhao, Z. K. (2007). "Efficient acid-catalyzed hydrolysis of cellulose in ionic liquid," *Advanced Synthesis and Catalysis* 349(11-12), 1847-1850. DOI: 10.1002/adsc.200700259
- Mandal, A., and Chakrabarty, D. (2011). "Isolation of nanocellulose from waste sugarcane bagasse (SCB) and its characterization," *Carbohydrate Polymers* 86(3), 1291-1299. DOI:10.1016/j.carbpol.2011.06.030
- Nada, A.-A. M., El-Kady, M. Y., El-Sayed, E. S. A., and Amine, F. M. (2009). "Preparation and characterization of microcrystalline cellulose (MCC)," *BioResources* 4(4), 1359-1371. DOI: 10.15376/biores.4.4.1359-1371
- Nazir, M. S., Wahjoedi, B. A., Yussof, A. W., and Abdullah, M. A. (2013). "Eco-friendly extraction and characterization of cellulose from oil palm empty fruit bunches," *BioResources* 8(2), 2161-2172. DOI: 10.15376/biores.8.2.2161-2172

- Nishiyama, Y., Langan, P., O'Neill, H., Pingali, S. V., and Harton, S. (2014). "Structural coarsening of aspen wood by hydrothermal pretreatment monitored by small- and wide-angle scattering of X-rays and neutrons on oriented specimens," *Cellulose* 21, 1015-1024. DOI 10.1007/s10570-013-0069-2
- Ohwoavworhwa, F. O., Adelakun, T. A., and Okhamafe, A. O. (2009). "Processing pharmaceutical grade microcrystalline cellulose from groundnut husk: Extraction methods and characterization," *International Journal of Green Pharmacy* 3, 97-104. DOI: 10.4103/0973-8258.54895
- Oyeniya, Y., and Itiola, O. (2012). "The physicochemical characteristic of microcrystalline cellulose, derived from sawdust, agricultural waste products," *International Journal of Pharmacy and Pharmaceutical Sciences* 4, 197-200.
- Pachua, L., Malsawmtluangi, C., Nath, N. K., Ramdinsangi, H., Vanlalfakawma, D. C., and Tripathi, S. K. (2013). "Physicochemical and functional characterization of microcrystalline cellulose from bamboo (*Dendrocalamus longispathus*)," *International Journal of PharmTech Research* 5(4), 1561-1571.
- Reddy, N., and Yang, Y. (2005). "Structure and properties of high quality natural cellulose fibers from cornstalks," *Polymer* 46, 5494-5500. DOI:10.1016/j.polymer.2005.04.073
- Rojas, J., Lopez, A., Guisao, S., and Ortiz, C. (2011). "Evaluation of several microcrystalline celluloses obtained from agricultural by-products," *Journal of Advanced Pharmaceutical Technology and Research* 2, 144-150. DOI:10.4103/2231-4040.85527
- Safinas, M. S. A., Bakar, A. A., and Ismail, H. (2013). "Properties of kenaf bast powder-filled high density polyethylene/ethylene propylene diene monomer composites," *BioResources* 8(2), 2386-2397. DOI: 10.15376/biores.8.2.2386-2397
- Shi, J., Shi, S. Q., Barnes, H. M., and Pittman, Jr., C. U. (2011). "A chemical process for preparing cellulosic fibers hierarchically from kenaf bast fibers," *BioResources* 6(1), 879-890. DOI: 10.15376/biores.6.1.879-890
- Sun, Y., Lin, L., Deng, H., Li, J., He, B., Sun, R., and Ouyang, P. (2008). "Structural changes of bamboo cellulose in formic acid," *BioResources* 3(2), 297-315. DOI: 10.15376/biores.3.2.297-315
- Thoorens, G., Krier, F., Leclercq, B., Carlin, B., and Evrard, B. (2014). "Microcrystalline cellulose, a direct compression binder in a quality by design environment—A review," *International Journal of Pharmaceutics* 473(1-2), 64-72. DOI:10.1016/j.ijpharm.2014.06.055
- Vanhatalo, K. M., and Dahl, O. P. (2014). "Effect of mild acid hydrolysis parameters on properties of microcrystalline cellulose," *BioResources* 9(3), 4729-4740. DOI: 10.15376/biores.9.3.4729-4740
- Wang, S., and Cheng, Q. (2009). "A novel process to isolate fibrils from cellulose fibers by high-intensity ultrasonication, Part 1: Process optimization," *Journal of Applied Polymer Science* 113(2), 1270-1275. DOI:10.1002/app.30072
- Wang, B., Sain, M., and Oksman, K. (2007). "Study of structural morphology of hemp fiber from the micro to the nanoscale," *Applied Composite Materials* 14(2), 89-103. DOI: 10.1007/s10443-006-9032-9
- Wang, D., Shang, S.-B., Song, Z.-Q., and Lee, M.-K. (2010). "Evaluation of microcrystalline cellulose prepared from kenaf fibers," *Journal of Industrial and Engineering Chemistry* 16(1), 152-156. DOI:10.1016/j.jiec.2010.01.003

- Wang, Q., Zhu, J., Gleisner, R., Kuster, T., Baxa, U., and McNeil, S. (2012). "Morphological development of cellulose fibrils of a bleached eucalyptus pulp by mechanical fibrillation," *Cellulose* 19(5), 1631-1643. DOI:10.1007/s10570-012-9745-x
- Wang, K., Yang, H., Chen, Q., and Sun, R.-C. (2013). "Influence of delignification efficiency with alkaline peroxide on the digestibility of furfural residues for bioethanol production," *Bioresource Technology* 146, 208-214. DOI:10.1016/j.biortech.2013.07.008
- Wyman, C. E., Decker, S. R., Himmel, M. E., Brady, J. W., Skopec, C. E., and Viikari, L. (2005). "Hydrolysis of cellulose and hemicellulose," *Polysaccharides: Structural Diversity and Functional Versatility* 1, 1023-1062. DOI:10.1201/9781420030822.ch43
- Zaini, L. H., Jonoobi, M., Tahir, P. M., and Karimi, S. (2013). "Isolation and characterization of cellulose whiskers from kenaf (*Hibiscus cannabinus* L.) bast fibers," *Journal of Biomaterials and Nanobiotechnology* 4(1), 37-44. DOI:10.4236/jbnb.2013.41006

Article submitted: December 14, 2015; Peer review completed: February 12, 2016; Revised version received: February 28, 2016; Accepted: February 29, 2016; Published: March 10, 2016.

DOI: 10.15376/biores.11.2.3875-3889